



Numerical investigation on the performance of an electrokinetic-based micromixer Equipped with circular-shaped electrodes

Elnaz Poorreza*¹

¹ Ph. D, Faculty of Electrical Engineering, University of Bonab, Bonab, Iran

ORCID: 0000-0003-0920-5208

elnaz.poorreza@gmail.com, e_poorreza@sut.ac.ir

ABSTRACT

Electroosmosis phenomena is drawing significant attention as a pumping and mixing means for use in microfluidic systems with the benefit of having simple structures and low-energy expenditure. An electroosmosis micromixer is a critical component inside microfluidic systems, which aims to efficiently mix the fluids at the microscale. These devices find applications across many scientific fields, including lab-on-chip devices, biomedical, medicine, etc. Electroosmosis can be described as fluid movement using micro/nano-channels due to an externally applied electric field. In the current work, an electroosmosis-driven micromixer has been designed that aims to mix two fluids. A sinusoidal electric potential is applied between the semi-circular electrodes, which has a peak value of 0.1 V with an operational frequency of 8 hertz. Simulation results derived using this arrangement reveal that the micromixer exhibits an impressive mixing efficiency with a value around 97%, thus indicating that the device has significant potential to be exploited for useful applications in an array of disciplines such as microfluidics, MEMS-based applications, and biomedical sciences.

Keywords: Microfluidic, Lab-on-Chips, Electroosmosis, Electrokinetic micromixer, MEMS

1. INTRODUCTION

Microfluidics is witnessing fast-paced growth with new developments finding numerous applications in the field of micro-sciences. After all, the advent and widespread application of microdevices like Lab-on-Chips (LoCs) and micro-total analysis systems (μ TASs), has brought microfluidics to the forefront [1]. Miniaturization of fluid functions has facilitated numerous benefits, including portability, the use of less reagent, quicker reactions, and the potential to be directly integrated with other microtechnologies, for example, sensors, electronics, and/or optics. Microfluidics, however, unlike the macroscale, typically involve laminar flow dynamics where the involved surface-to-volume ratios are high. In the case of laminar flows, efficient mixing of fluid species is an important challenge due to the low advection that naturally exists in microchannels. Unaided mixing of microfluids is thus left to depend on the slow process of diffusion [2-9]

Micromixers are widely utilized in applications including bioprocess equipment, medical devices, and chemical processing, to ensure effective mixing and miniaturization processes. Rapid mixing of large biological molecules, like proteins, DNA, and different biofluids, has received a lot of attention in the field of biotechnology. Mixing of different fluids at the microscopic devices can be attained through active and passive methods. These classifications are based upon the nature of mixing that takes place at the microsystems [10, 11]. Microfluidics micromixers are categorized into two key types, active and passive micromixers, based on the external energy supply that operates. Active micromixers utilize external sources such as electric fields, acoustic fields, magnetic fields, and photothermal effects to operate and control the mixing fluids [12]. These sources produce disturbance inside the flow fluid, leading to the improvement of heterogeneous fluid species transport [13]. Such a kind of disturbance improves the interfacial area between



two different fluids. Furthermore, the basic advantages of using the active actuation approach are higher mixing, which is best appropriate for precise control, and a complex mixing pattern for various biofluids and chemicals [12, 14]. Among the micromixing devices with the benefit of simplicity, no moving components, and ease of integration with microelectrodes, the active electrokinetically driven micromixers are more appealing and are under wide research studies.

In this work, an electroosmotic micromixer has been designed to mix two different fluids. A sinusoidal electric potential is repeatedly applied to the semi-circular electrodes, which are defined by the peak value of 0.1 V and the operation frequency of 8 hertz. Simulation results obtained based on this setup indicate that the micromixer has an exemplary mixing efficiency of close to 97%, thus highlighting the enormous potential of the device toward beneficial applications to a broad range of fields, including the area of microfluidics, biochemistry, and biomedical science.

2. GOVERNING EQUATIONS

For simulating the electroosmotic micromixing, the flow field is solved based on the continuity and Navier-Stokes equations. The Navier-Stokes equations of the incompressible flow simulate the flow inside the channels as follows [15]:

$$\rho \frac{\partial \mathbf{u}}{\partial t} - \nabla \cdot \eta (\nabla \mathbf{u} + (\nabla \mathbf{u})^T) + \rho \mathbf{u} \cdot \nabla \mathbf{u} + \nabla p = 0 \quad (1)$$

$$\nabla \cdot \mathbf{u} = 0$$

Here η signifies the dynamic viscosity (SI unit: kg/(m·s)), u expresses the velocity (SI unit: m/s), ρ corresponds to the fluid density (SI unit: kg/m³), and p indicates to the pressure (SI unit: Pa). The mixed fluid flows freely are out of the right end boundary, where can be specified vanishing total stress components normal to the boundary:

$$\mathbf{n} \cdot [-p\mathbf{I} + \eta (\nabla \mathbf{u} + (\nabla \mathbf{u})^T)] = 0 \quad (2)$$

When brought into contact with an electrolyte, the majority of solid substrates display an electrostatic surface charge. As a response to the spontaneous surface charge, an electrolyte phase carrying the charge forms near the liquid-solid interface. An electric double layer is formed owing to the availability of the charged objects at the surface that share contact with the nearby solution. Under the application of an external electric field, the resulting electroosmotic flow provides the driving potential for the displacement of the charged liquid inside the confines of the electric double layer. This device uses a force on the positively charged liquid nearby to the wall surface, thereby instigating fluid motion in the direction associated with the electric field. The velocity gradients that are perpendicular to the wall facilitate viscous transport within this particular orientation. In the absence of opposing forces, the velocity profile eventually converges towards the state of nearly uniformity throughout the cross-sectional area that is perpendicular to the wall. This theoretical model replaces the thin electric double-layer concept with the Helmholtz-Smoluchowski equation, which defines the relationship between electroosmotic velocity and the tangent component of the applied electric field [16].

$$\mathbf{u} = \frac{\varepsilon_w \zeta_0}{\eta} E_t \quad (3)$$

$$E_t = E - (E \cdot \mathbf{n})\mathbf{n}$$

In this equation, $\varepsilon_w = \varepsilon_0 \varepsilon_r$ is the electric permittivity of fluid (F/m), ζ_0 indicates the zeta potential at the channel wall. E_t shows the tangential component of the electric field (E) at the interface between the fluid and a charged surface. E signifies the total electric field vector. \mathbf{n} indicates the unit normal vector

This Equation holds good throughout all the boundaries with the only exceptions at the entrance and the exit. Assuming that no gradients exist for the ions that cause the current to be carried, it is possible to describe the balance of the current inside the channel based upon Ohm's law, along with the current density balance equation [15]:

$$\nabla \cdot (-\sigma \nabla V) = 0 \quad (4)$$

where σ indicates conductivity (S/m) and the expression within parentheses displays the current density (A/m²)

The sinusoidal electric potentials applied on the electrodes, with the same maximum value ($V_0 = 0.1$ V) and the same frequency (8 Hz), but they alternate in polarity. The potentials on the electrodes are $\mp V_0 \sin(2\pi ft)$ (f represents the signal frequency and t is the time), (see Figure 1). All other boundaries of the

mixer are insulated. The insulation boundary condition sets the normal component of the electric field to zero.

$$-\sigma \nabla V \cdot \mathbf{n} = 0 \quad (5)$$

In the upper half of the inlet of micromixer (Figure 1), the concentration of the fluid is defined as c_0 ; conversely, in the lower half of the inlet, the concentration is set to zero. Therefore, the concentration exhibits a sharp transition from zero to c_0 at the middle of the inlet boundary. The mixed solution drains out of the right outlet through convective flow, whereas all the remaining boundaries are considered to be insulated. Inside the channel, the following one-dimensional convection-diffusion equation explains the solute concentration inside the fluid:

$$\frac{\partial c}{\partial t} + \nabla \cdot (-D \nabla c) = R - \mathbf{u} \cdot \nabla c \quad (6)$$

In this equation, c signifies the concentration, D indicates the diffusion coefficient, R is the reaction rate, ∇c shows the gradient of concentration, and \mathbf{u} demonstrates the flow velocity. In this model, R is set to zero, as the concentration remains unaffected by any chemical reactions.

To assess the degree of mixing, or to improve mixing performance, the mixing efficiency, Q , at any cross-section of the microchannel is quantified by Equation 7 [17].

$$Q = \left[1 - \frac{\int |c - c_\infty| d_A}{\int |c_0 - c_\infty| d_A} \right] \times 100\% \quad (7)$$

Where, c signifies the species concentration across the width of the micromixer, c_∞ directs the species concentration in the completely mixed state (i.e. = 0.5), and c_0 is species concentration in the completely unmixed condition (i.e. $c_0 = 0$ or 1).

3. MODEL GEOMETRY

Figure 1 indicates the schematic of the intended micromixer. An electric potential of 0.1 V with a frequency of 8 Hz that is supplied to the electrodes. The reason behind the use of the frequency of 8 Hz, is based on the recent studies [18]. Generally, mixing is higher with escalation of the field parameters like the frequency and applied voltage. Results are affected due to variation of the field frequency. Mixing efficiency may be dependent on the actuation frequency under the use of an alternating field. This is due to the fact that chaotic mixing is not possible under low Reynolds number flows due to the lack of turbulence, yet the electric frequency is capable of flipping the flow between the stable to unstable regions to generate a mixing force. The semi-circular radius of the electrodes is 5 μm . Three physics of Laminar Flow, Electric currents, and transport of diluted species were integrated to simulate the scenario. Fig. 2 indicates the boundary conditions impressed according to the governing equations subsection. Fluid properties are described in Table 1. Figure 3 depicts the mesh arrangement of the micromixer. To mesh the proposed setup, free triangular domains are chosen. The total mesh covers 5300 domain elements and 268 boundary elements

Table 1. Properties of the micromixer [19, 20]

Parameter	Value	Description
ρ	1000 Kg/m ³	fluid Density
η	10 ⁻³ Pa.s	Dynamic viscosity of the fluid
U_0	0.1 mm/s	Average velocity of the inlet
ϵ_r	80.2	Relative electric permittivity of the fluid
ζ	-0.1 V	Zeta potential on the wall-fluid boundary
σ	0.118[S/m]	Conductivity of the ionic solution
D	10 ⁻¹¹ m ² /s	Diffusion coefficient
c_0	1 mol/ m ³	Initial concentration

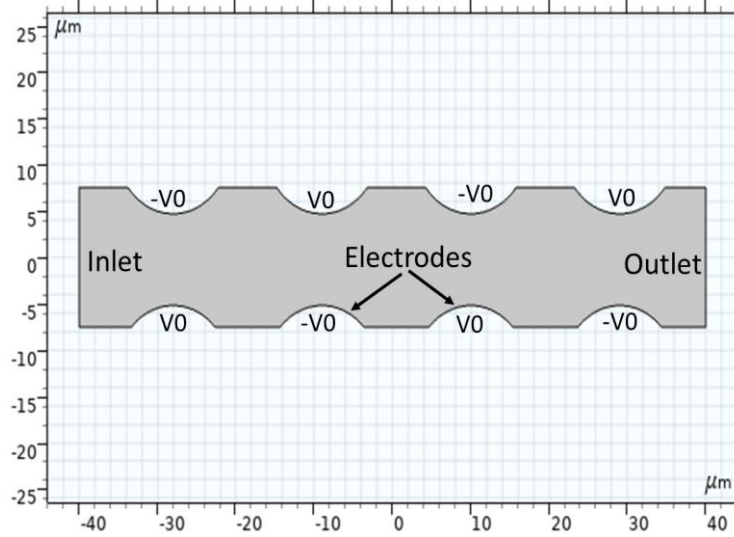


Fig. 1. Schematic view of micromixer with symmetric electrodes on the wall of the mixing chamber

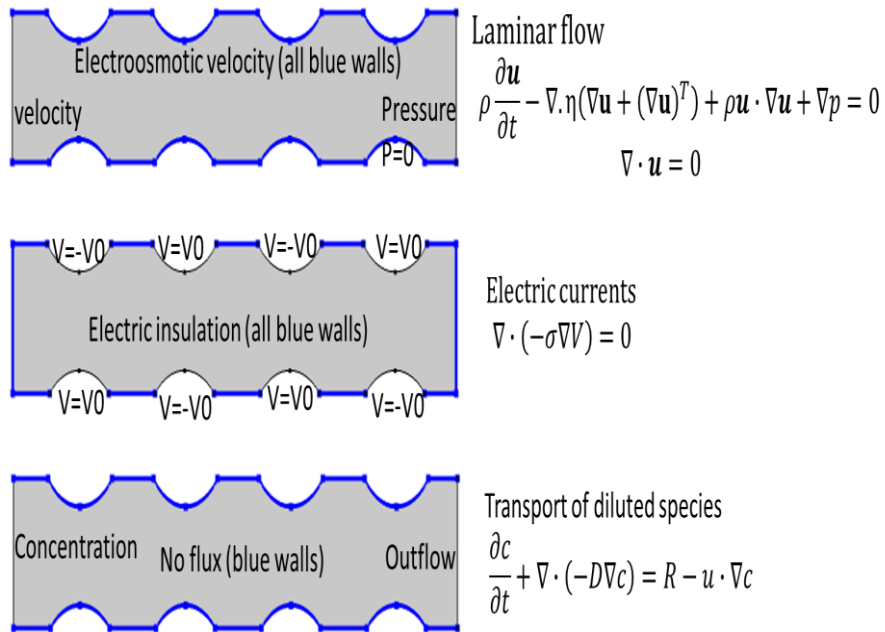


Fig. 2. applied boundary conditions

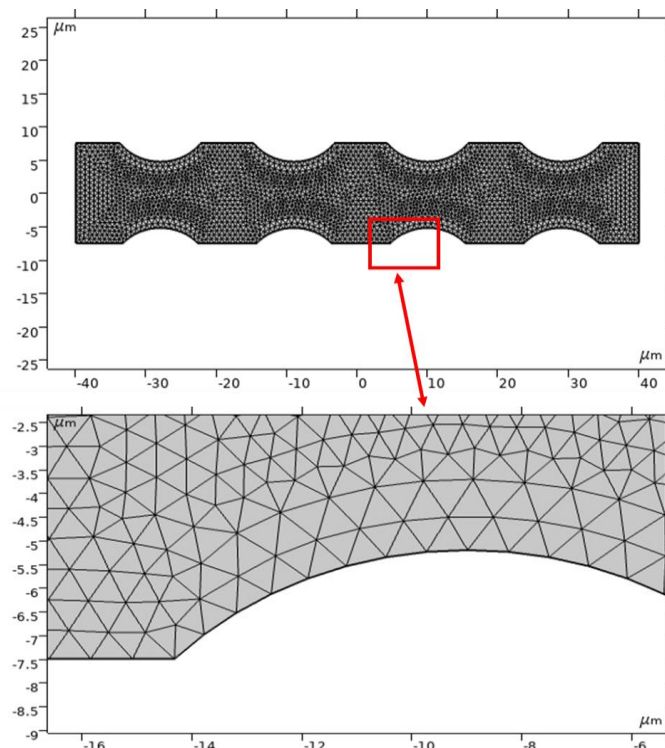


Fig.3. Mesh set-up

4. RESULTS AND DISCUSSION

Figure 4 indicates the characteristic streamline distribution in the micromixer at (a) $t = 0$ s (no excitation) and (b), $t = 0.41$ s, the moment at which the alternating electric field attains the highest magnitude. It indicates that electroosmotic recirculation of the fluid strongly agitates the flow, typically in the shape of rotating vortices located near the electrodes. The basic mechanisms responsible for efficient mixing include an interaction of repeated stretching and folding up of fluid pieces along with the diffusion at infinitesimal scales. Figures 5(a), (b) shows the plot of electric potential ($\pm V_0$) and electric field for the electroosmotic micromixer respectively. As it is clear the maximum value of electric potential and electric field distribution are near the electrodes.

Figure 6(a) depicts the steady-state concentration when there is no electric field present. It is characterized as a laminar flow, where the coefficient of diffusion is very low; therefore, the two fluids are still well separated at the exit. However, after the application of the alternating electric field, it can be observed that an enhanced mixing has occurred, which is due to the alternating vortices that exist inside the flow. Figures 6(b), (c), and (d) depict the system at different mixing times. Fig. 6(c) indicates the concentration profile when both the electric field and the electroosmotic velocity attain their peak values during the cycle (at $|\sin \omega t| = 1$).

For computation of the mixing efficiency and the concentration, the red cross-section indicated in Fig 7(a), located close to the outlet, is utilized. Figure 7(b) depicts the profiles of the concentrations at the outlet of the microchannel at several time points (as indicated in the legend of the figure). Figure 7(c) depicts the mixing efficiency along the cross-section of the channel, measured at several time points, which are further indicated in the legend of the figure, thus providing an overall idea of the mixing processes happening inside the microchannel at different moments. It can be noted that due to the random nature of the perturbation, the mixing efficiency profile is not of uniform nature. These results validate that high mixing efficiency can be achieved with the designed mixer under this study. Based on Equation (7), the mixing efficiency of the fluids approaches nearly 97%.

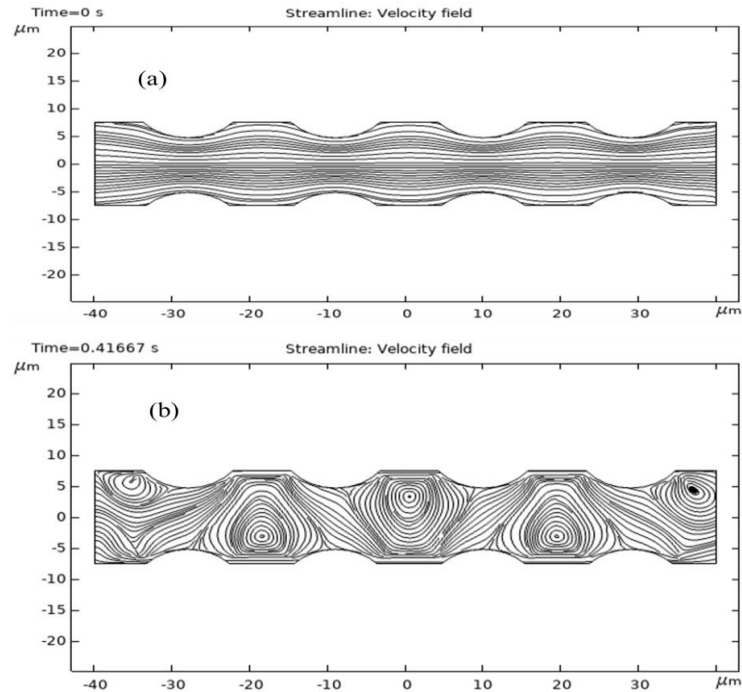


Fig. 4. Fluid streamlines in an electroosmotic micromixer at (a) $t = 0$ s (no excitation), (b), $t = 0.4166$ s, when the alternating electric field has its largest magnitude.

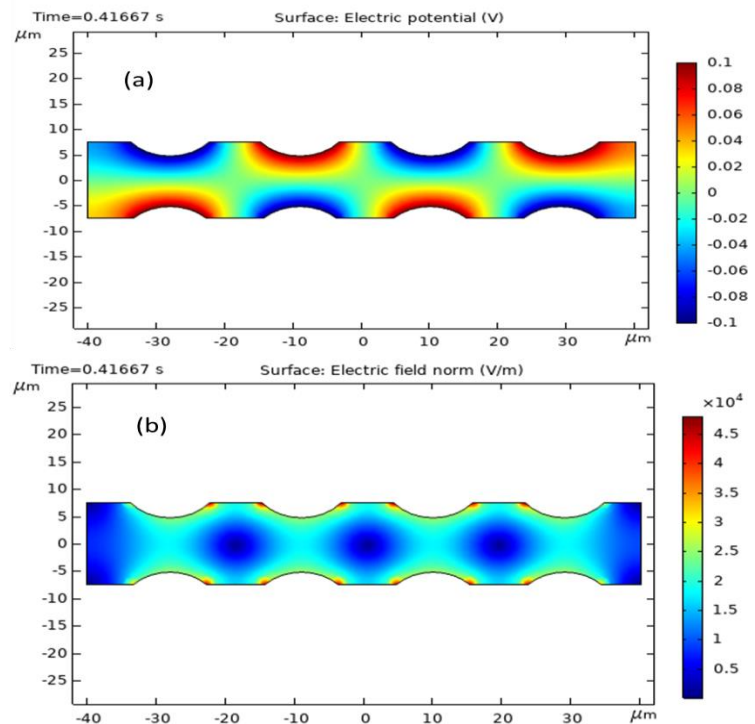


Fig. 5. (a) profile of electric potential ($\pm V_0$) for the electroosmotic micromixer (b) and electric field at $t = 0.41$ s.

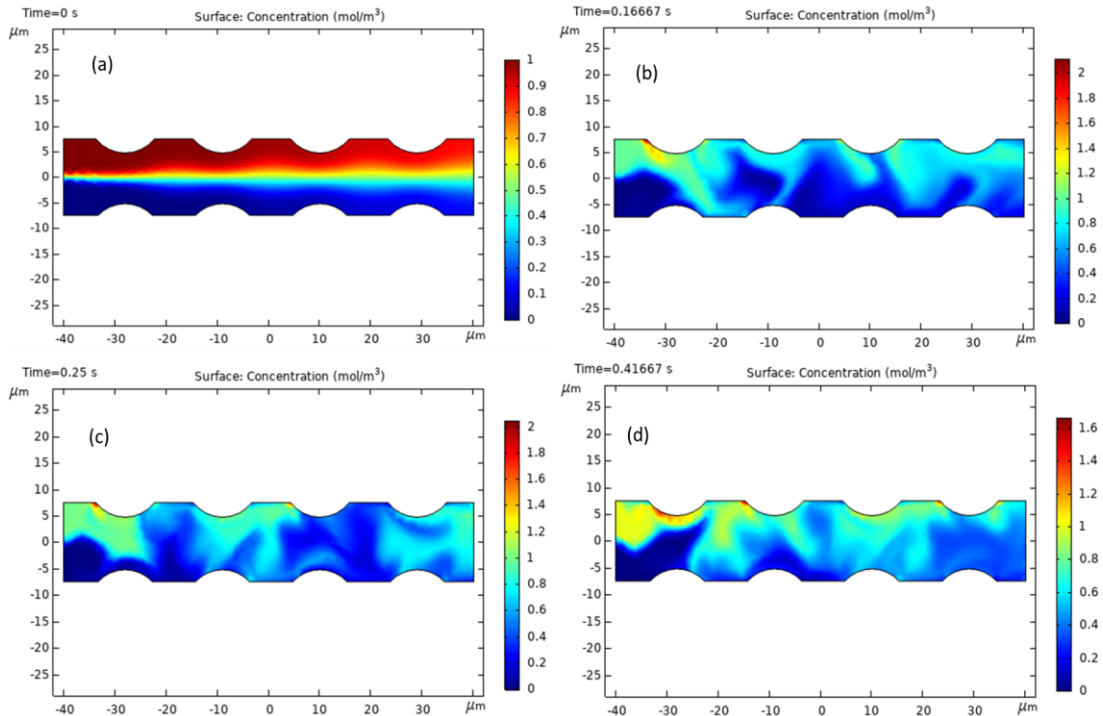


Fig. 6. Concentration plot of the micromixer: (a) time = 0 s, (Steady-state solution in the absence of an electric field) (b), time = 0.08 (c) time: 0.25s, and (d) time: 0.41s.

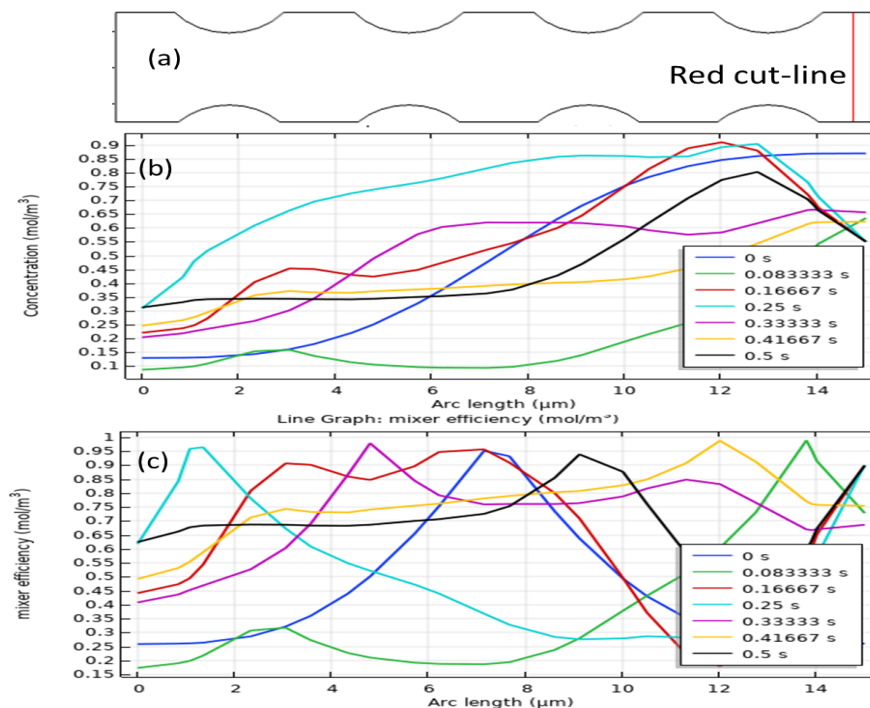


Fig. 7. (a) Species concentration plots at the outlet of the microchannel at different times (shown in the figure legend) (b) Mixing index across the cross-section of the channel at different times.

CONCLUSION

In the current work, an electroosmosis-driven micromixer has been designed to achieve the mixing of two different fluids. A sinusoidal electric potential of peak amplitude 0.1 V at the frequency of 8 hertz is intentionally applied between the semi-circular electrodes. Simulation results obtained through this setup are indicative of the fact that the micromixer has an excellent mixing efficiency close to 97%, thus highlighting its vast potential for beneficial use in a vast array of applications, especially those related to microfluidics, biochemistry, and biomedical sciences.

REFERENCES

- [1] J. Zhou, Y. Tao, R. Xue, and Y. Ren, (2023). A Self-Powered Dielectrophoretic Microparticle Manipulation Platform Based on a Triboelectric Nanogenerator, *Advanced Materials*, vol. 35, no. 1, p. 2207093.
- [2] S. M. Saravanakumar, M. Jamshidi Seresht, R. Izquierdo, and P.-V. Cicek. A novel DC electroosmotic micromixer based on helical vortices, in *Actuators*, 2024, vol. 13, no. 4: MDPI, p. 139.
- [3] S. M. Saravanakumar and P.-V. Cicek, (2023) Microfluidic mixing: A physics-oriented review," *Micromachines*, vol. 14, no. 10, p. 1827.
- [4] A. Nikiforov, E. Lazareva, E. Edemskaya, V. Semenov, K. Gareev, and D. Korolev, (2024). Microfluidic synthesis of magnetite nanoparticles and its comparison with synthesis in a batch reactor, *Colloid Journal*, vol. 86, no. 4, pp. 547-558.
- [5] A. Malick and B. Barman, (2024) Electroosmotic Flow Modulation through Soft Nanochannel Filled with Power-law Fluid under Impacts of Ion Steric and Ion Partitioning Effects," *Colloid Journal*, vol. 86, no. 4, pp. 610-626.
- [6] E. Poorreza and H. B. Ghavifekr, (2021). Experimental and Simulation Investigations of Magnetic Liquid Marble Manipulation with a Permanent Magnet, *Colloid Journal*, vol. 83, no. 6, pp. 752-762.
- [7] D. Bahrami, A. A. Nadooshan, and M. Bayareh, (2022) Effect of non-uniform magnetic field on mixing index of a sinusoidal micromixer, *Korean Journal of Chemical Engineering*, pp. 1-12.
- [8] L. Smirnov and T. Kulagina, (2017). Features of the kinetics of chemical reactions in a nanostructured liquid, *Russian Journal of Physical Chemistry B*, vol. 11, pp. 786-797.
- [9] A. Valov and V. Avetisov, (2022) "Fluctuational Features of Diffusive Passage of Particles in Narrow Channels with Obstacles," *Russian Journal of Physical Chemistry B*, vol. 16, no. 3, pp. 474-478.
- [10] B. Gayen, N. K. Manna, and N. Biswas, (2024). Enhancing mixing performance in a square electroosmotic micromixer through an off-set inlet and outlet design, *Physics of Fluids*, vol. 36, no. 6.
- [11] Y.-J. Xu et al., (2021). Electro-osmotic flow of biological fluid in divergent channel: drug therapy in compressed capillaries, *Scientific reports*, vol. 11, no. 1, p. 23652.
- [12] M. Waqas, G. Janusas, V. Naginevičius, and A. Palevicius, (2024) The Design and Investigation of Hybrid a Microfluidic Micromixer, *Applied Sciences*, vol. 14, no. 12, p. 5315.
- [13] C. Bai, W. Zhou, S. Yu, T. Zheng, and C. Wang, (2022) "A surface acoustic wave-assisted micromixer with active temperature control, *Sensors and Actuators A: Physical*, vol. 346, p. 113833.
- [14] M. Waqas, A. Palevicius, V. Jurenas, K. Pilkauskas, and G. Janusas, (2025). Design and Investigation of a Passive-Type Microfluidics Micromixer Integrated with an Archimedes Screw for Enhanced Mixing Performance, *Micromachines*, vol. 16, no. 1, p. 82.
- [15] A. Agarwal, A. Salahuddin, H. Wang, and M. J. Ahamed, (2020) Design and development of an efficient fluid mixing for 3D printed lab-on-a-chip, *Microsystem Technologies*, vol. 26, no. 8, pp. 2465-2477.
- [16] X. Niu and Y.-K. Lee, (2003). Efficient spatial-temporal chaotic mixing in microchannels," *Journal of Micromechanics and microengineering*, vol. 13, no. 3, p. 454.
- [17] R. H. Vafaie, M. Mehdipoor, A. Pourmand, E. Poorreza, and H. B. Ghavifekr, (2013) An electroosmotically-driven micromixer modified for high miniaturized microchannels using surface micromachining, *Biotechnology and bioprocess engineering*, vol. 18, no. 3, pp. 594-605.
- [18] H. Chen, Y. Zhang, I. Mezic, C. Meinhart, and L. Petzold, Numerical simulation of an electroosmotic micromixer, in *ASME International Mechanical Engineering Congress and Exposition*, 2003, vol. 37165, pp. 653-658.



- [19] N. J. Ghahfarokhi, M. Bayareh, A. A. Nadooshan, and S. Azadi, (2021) "Mixing enhancement in electroosmotic micromixers, *Journal of Thermal Engineering*, vol. 7, no. 2, pp. 47-57,.
- [20] M. Nazari, P.-Y. A. Chuang, J. A. Esfahani, and S. Rashidi, (2020) *A comprehensive geometrical study on an induced-charge electrokinetic micromixer equipped with electrically conductive plates, International Journal of Heat and Mass Transfer*, vol. 146, p. 118892,.